

Journal Pre-proofs

Research paper

Synthesis, Characterization and Study on the Dissimilar Reactivity of a Ni(II)–Bis(Iminosemiquinone) Complex Core to Ligand–Appended Hemilabile –CH₂OH and –CH₂NH₂ Units

Prasenjit Sarkar, Samir Ghorai, Ganesh Chandra Paul, Mahmuda Khannam, Surajit Barman, Chandan Mukherjee

PII: S0020-1693(19)31106-5
DOI: <https://doi.org/10.1016/j.ica.2019.119340>
Reference: ICA 119340

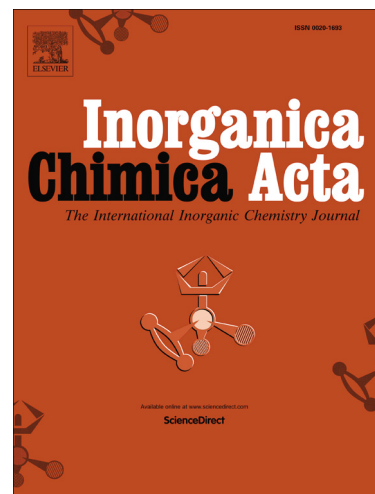
To appear in: *Inorganica Chimica Acta*

Received Date: 30 July 2019
Revised Date: 26 October 2019
Accepted Date: 2 December 2019

Please cite this article as: P. Sarkar, S. Ghorai, G. Chandra Paul, M. Khannam, S. Barman, C. Mukherjee, Synthesis, Characterization and Study on the Dissimilar Reactivity of a Ni(II)–Bis(Iminosemiquinone) Complex Core to Ligand–Appended Hemilabile –CH₂OH and –CH₂NH₂ Units, *Inorganica Chimica Acta* (2019), doi: <https://doi.org/10.1016/j.ica.2019.119340>

This is a PDF file of an article that has undergone enhancements after acceptance, such as the addition of a cover page and metadata, and formatting for readability, but it is not yet the definitive version of record. This version will undergo additional copyediting, typesetting and review before it is published in its final form, but we are providing this version to give early visibility of the article. Please note that, during the production process, errors may be discovered which could affect the content, and all legal disclaimers that apply to the journal pertain.

© 2019 Published by Elsevier B.V.



Synthesis, Characterization and Study on the Dissimilar Reactivity of a Ni(II)–Bis(Iminosemiquinone) Complex Core to Ligand–Appended Hemilabile –CH₂OH and –CH₂NH₂ Units

Prasenjit Sarkar,[‡] Samir Ghorai,[‡] Ganesh Chandra Paul, Mahmuda Khannam, Surajit Barman, and Chandan Mukherjee*

Department of Chemistry, Indian Institute of Technology Guwahati, Guwahati, 781039, Assam, India; Corresponding author, email: cmukherjee@iitg.ac.in

[‡] Contributed equally.

Abstract

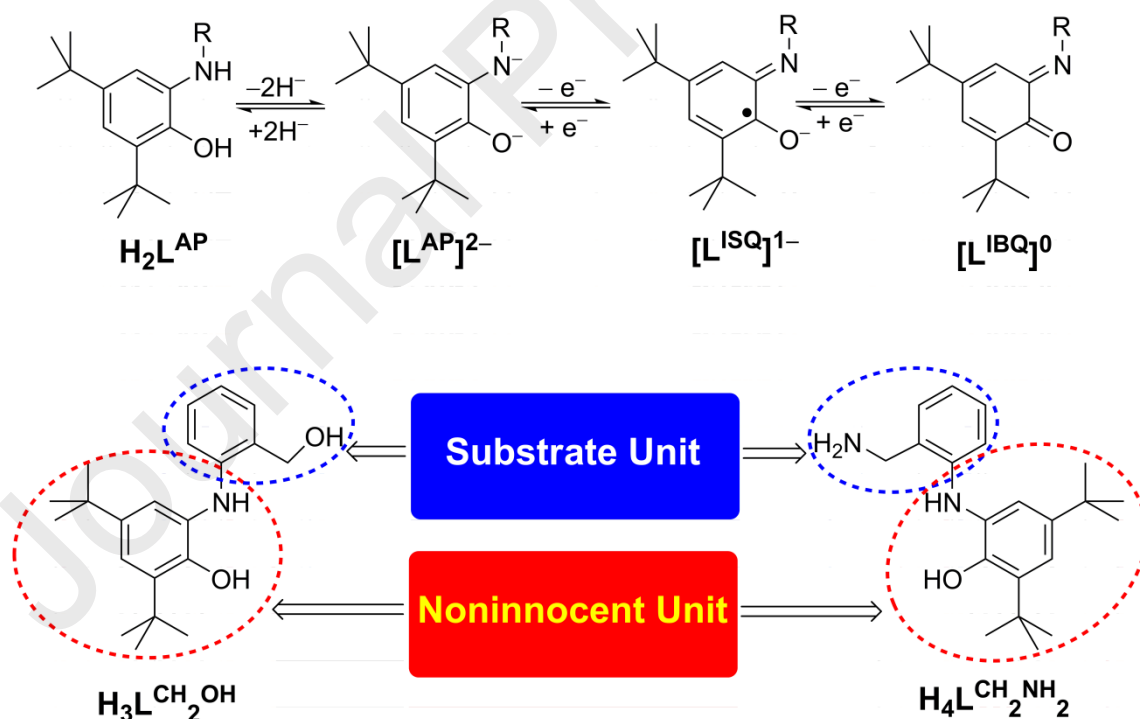
Noninnocent ligand H₃L^{CH₂OH} reacted with NiCl₂•6H₂O under aerial atmosphere and provided corresponding complexes **1** {[Ni^{II}(HL^{CH₂OH})₂]⁰} and **1a** {[Ni^{II}(L^{CHO})₂]⁰} in the presence of Et₃N and NaOH, respectively. Ligand H₄L^{CH₂NH₂} provided complex **2** {[Ni^{II}(HL³)⁰} in the presence of NiCl₂•6H₂O and Et₃N under air. All the complexes were characterized by various spectroscopic and spectrometric techniques, which included FT-IR, mass, UV–vis/NIR, ¹H NMR, cyclic voltammetry and single crystal X–ray diffraction methods. Molecular structural analyses on complexes **1** and **1a** revealed that both four-coordinate complexes were neutral in charge and consisted of two ligand–centered iminosemiquinone radicals and a Ni(II) ion. While, the hemilabile –CH₂OH group remained unaffected and did not make any coordination with the central Ni(II) ion in complex **1**, two-electron oxidation of each –CH₂OH group to –CHO group was realized in complex **1a**. In complex **2**, the ligand backbone was an innocent tetradentate salen unit, which was formed by a complete modification of the initial noninnocent ligand H₄L^{CH₂NH₂}. To find out the mechanistic path for the formation of complex **2**, ligand H₃L1 and H₄L2 were also introduced and it was presumed that transimination took place in the ligand backbone during complex **2** formation.

Keywords

Redox noninnocent ligands; Ni(II)–radical complexes; antiferromagnetic coupling; cyclic voltammetry; oxidation of alcohols.

Introduction

Redox noninnocent ligands-coordinated transition metal complexes are widely under investigation as redox catalysts. [1-6] Bidentate 2-aminophenol derivatives (H_2L^{AP} ; Scheme 1) have been recognized as noninnocent ligands [7-15] and have been identified to exist in its various oxidation states in the corresponding coordination metal complexes as shown in Scheme 1. Some of the complexes have been exclusively studied as redox catalysts. [1-6] For instances: radical(s)-containing Cu(II) complexes have been employed for the aerial oxidation of primary alcohols to the corresponding aldehydes as well as for the aziridination of vinylic substrates; [16, 17] using four-coordinate Pd(II)-aminophenolate and five-coordinate Fe(III)-iminosemiquinone complexes, C-H amination reactions of several azide compounds are reported to occur *via* the initial nitrene radical intermediates formation [18, 19]; Desage-El Murr and coworkers have reported an electron transfer from a Ni(II)-coordinated iminosemiquinone unit to $[CF_3]^+$ and the consequent generation of $[CF_3]^{\bullet}$ radical, which undergoes C-C bond formation with either indole- or vinyl silyl ether-based substrates in a catalytic reaction. [20]



Scheme 1. Top: the possible various oxidation states of 2-aminophenol derivatives. AP = amidophenolate; ISQ = iminosemiquinone; and IBQ = iminobenzoquinone. Bottom: Ligands with the designation of the substrate unit and the noninnocent unit.

In continuation of our understanding on reactivity of transition metal–radical complexes, we investigated two ligands $H_3L^{CH_2OH}$ and $H_4L^{CH_2NH_2}$, which were comprised of a noninnocent 2–amino–4,6–di–*tert*–butylphenol unit to generate a metal-coordinated ligand–based radical; and either a benzyl alcohol or a benzyl amine hemilabile unit in the ligand backbone as the substrate (Scheme 1). We intended to realize the reactivity difference between benzyl alcohol and benzyl amine units under the same chemical and geometrical environment. In this context, we study Ni(II) ions because Ni(II) would provide four–coordinate complexes. Thus, two axial positions would be available for the hemilabile units to establish weak interactions and thereafter, the units would undergo electron–transfer reactions with the Ni(II)–coordinated radical centers as observed in other radical–containing metal complex catalyses. [3, 4, 21]

Noninnocent ligand $H_3L^{CH_2OH}$ [22] reacted under air with $NiCl_2 \cdot 6H_2O$ and provided four–coordinate, neutral Ni(II)–bis(iminosemiquinone) complexes **1** and **1a** in the presence of Et_3N and NaOH, respectively. In complex **1a** the ligand–centered benzyl alcohol unit underwent oxidation to benzaldehyde unit. Additionally, complex **1**, which contained benzyl alcohol in the ligand backbone, could also be transformed into **1a** in the presence of NaOH in CH_3OH . Contrary to ligand $H_3L^{CH_2OH}$, ligand $H_4L^{CH_2NH_2}$ [23] provided complex **2** in the presence of $NiCl_2 \cdot 6H_2O$ and Et_3N under air. In the complex, the ligand backbone was an innocent tetradentate salen unit, which was formed by a complete modification of the initial noninnocent ligand $H_4L^{CH_2NH_2}$. The complexes were characterized by FT–IR, mass, UV–vis/NIR, 1H NMR spectroscopic techniques, and X–ray diffraction technique and reported in this work. In addition, possible routes for the formation of complex **1a** and **2** were also incorporated.

Experimental Section

Materials: All the chemicals and solvents were obtained from commercial sources and were used as supplied, unless noted otherwise. The 3,5–di–*tert*–butylcatechol, 2–aminobenzonitrile, 2–aminobenzylamine, and 2–aminobenzylalcohol, were purchased from Sigma–Aldrich. Solvents were obtained from Merck (India). Mass spectra were measured in HPLC-grade acetonitrile solution.

Physical measurements: X-ray crystallographic data were collected using a SuperNova, (Single source at offset, Eos) diffractometer, equipped with a sealed tube Mo-K α radiation ($\lambda = 0.71073 \text{ \AA}$). Structures were solved with the Superflip, structure solution program using Charge Flipping and refined by direct methods using SHELXS-97 or SHELXS-2013 and with full-matrix least squares on F^2 using SHELXL-97. [24] All the non-hydrogen atoms were refined anisotropically. IR spectra were recorded on Perkin Elmer Instrument at normal temperature by making KBr pellet (grinding the sample with IR-grade KBr). Mass spectral data were obtained from Q-TOF MS Spectrometer. UV-Vis-NIR spectra were recorded on Perkin Elmer, Lamda 750, UV-Vis-NIR spectrometer, preparing a known concentration of the samples in HPLC Grade CH₂Cl₂ at room temperature using cuvette of 1 cm width. ¹H-, and ¹³C-NMR spectra of the ligand and complexes were recorded in 'Varian Mercury plus 400 MHz NMR machine at 298 K. X-band EPR spectra were examined on JEOL, JES-FA200 machine. Cyclic voltammograms (CVs) of the complexes (1 mM) were being recorded on VersaSTAT 3 instrument in CH₂Cl₂ solutions containing 0.10 M [(ⁿBu)₄N]ClO₄ as supporting electrolyte. A glassy carbon working electrode, a platinum wire counter electrode, and a Ag/AgCl reference electrode were used for the measurements. Ferrocene was used as an internal standard, and herein, all the potentials are referenced *versus* the ferrocenium/ferrocene (Fc⁺/Fc) couple. The number of electron transfer was determined by comparing peak current.

Table 1: Crystallographic parameters and refinement data for complexes **1**, **1a** and **2**.

	Complex 1	Complex 1a	Complex 2
Empirical formula	C21 H27 N Ni0.50 O2	C42 H50 N2 Ni O4	C28 H31 N3 Ni O
Formula weight	354.79	705.55	484.27
CCDC Number	1943217	1943218	964880
Crystal habit, colour	Block, green	Block, green	Needle, brown
Crystal size, mm ³	0.35 × 0.34 × 0.30	0.33 × 0.30 × 0.28	0.46 × 0.22 × 0.18
Temperature, T	102(3)	293(2)	296(2)
Wavelength, λ (Å)	0.71073	0.71073	0.71073
Crystal system	triclinic	triclinic	monoclinic
Space group	' P -1'	' P -1'	' C 2/c'
Unit cell dimensions	$a = 5.7899(8) \text{ \AA}$ $b = 12.5127(9) \text{ \AA}$ $c = 13.9208(14) \text{ \AA}$ $\alpha = 71.193(8)^\circ, \beta = 80.081(10)^\circ$ $\gamma = 81.402(8)^\circ$	$a = 6.6721(3) \text{ \AA}$ $b = 14.0949(8) \text{ \AA}$ $c = 21.7775(10) \text{ \AA}$ $\alpha = 104.148(4)^\circ, \beta = 92.361(4)^\circ$ $\gamma = 93.747(4)^\circ$	$a = 25.810(2) \text{ \AA}$ $b = 6.9366(6) \text{ \AA}$ $c = 28.778(3) \text{ \AA}$ $\alpha = \gamma = 90^\circ, \beta = 96.065(8)^\circ$

Volume, V (Å ³)	935.62(18)	1978.18(17)	5123(8)
Z	2	2	8
Calculated density, Mg·m ⁻³	1.259	1.185	1.256
Absorption coefficient, μ (mm ⁻¹)	0.562	0.531	0.781
$F(000)$	380	752	2048
θ range for data collection	2.65° to 24.99°	2.72° to 24.99°	3.04° to 25.00°
Limiting indices	$-6 \leq h \leq 6, -14 \leq k \leq 14,$ $-16 \leq l \leq 16$	$-6 \leq h \leq 7, -16 \leq k \leq 9,$ $-22 \leq l \leq 25$	$-29 \leq h \leq 30, -8 \leq k \leq 7,$ $-29 \leq l \leq 34$
Reflection collected/unique	6216/5759 [R(int)=0.0285]	13348/6933 [R(int)=0.0468]	9287/4511 [R(int)=0.0565]
Completeness to θ	99.7% ($\theta = 25.00^\circ$)	99.9% ($\theta = 25.00^\circ$)	99.9% ($\theta = 25.00^\circ$)
Max. and min. transmission	0.821/0.845	0.839/0.862	0.869/0.814
Refinement method	'SHELXL-2013'	'SHELXL-2013'	Full-matrix least-squares on F^2
Data/restraints/parameters	3293/0/230	6933/0/457	4511/0/304
Goodness-of-fit on F^2	1.046	1.068	1.030
Final R indices [$I > 2\sigma(I)$]	$R1 = 0.0823, wR2 = 0.1987$	$R1 = 0.0667, wR2 = 0.1399$	$R1 = 0.0557, wR2 = 0.1166$
R indices (all data)	$R1 = 0.1150, wR2 = 0.2278$	$R1 = 0.1256, wR2 = 0.1737$	$R1 = 0.0994, wR2 = 0.1439$
Largest diff. peak and hole	1.073 and -0.486 e·Å ⁻³	0.436 and -0.354 e·Å ⁻³	0.302 and -0.440 e·Å ⁻³

Syntheses

Synthesis of [C₄₂H₅₄N₂NiO₄]; **1; {[Ni^{II}(HL^{CH₂OH})₂]⁰}: A mixture containing ligand H₃L^{CH₂OH} (0.329 g, 1.0 mmol) and NiCl₂·6H₂O (0.119 g, 0.5 mmol) in acetonitrile (15mL) was stirred for 10 minutes under air at room temperature (30 °C). Triethylamine (0.2 mL) was added to the reaction mixture. After that, the resulting solution was refluxed for 2 h. The solution was cooled to room temperature. Then the reaction mixture was filtered to obtain a green solid. The obtained residue was recrystallized from dichloromethane:acetonitrile (3:1) solvent mixture by slow solvent evaporation that led to the X-ray quality single crystal. Yield: 0.183g, 0.26 mmol, 52%. Fourier transform infrared (FTIR) (KBr pellet, cm⁻¹): 3556, 3437, 2957, 2905, 2867, 1631, 1533, 1459, 1359, 1321, 1257, 1228, 1199, 1174, 1107, 1040, 914, 745. ¹H NMR (CDCl₃, 399.85 MHz): δ 0.99 (s, 18H, ^tBu), 1.06 (s, 18H, ^tBu), 2.07 (s, 1H, -OH), 2.31 (s, 1H, -OH), 4.72–5.01**

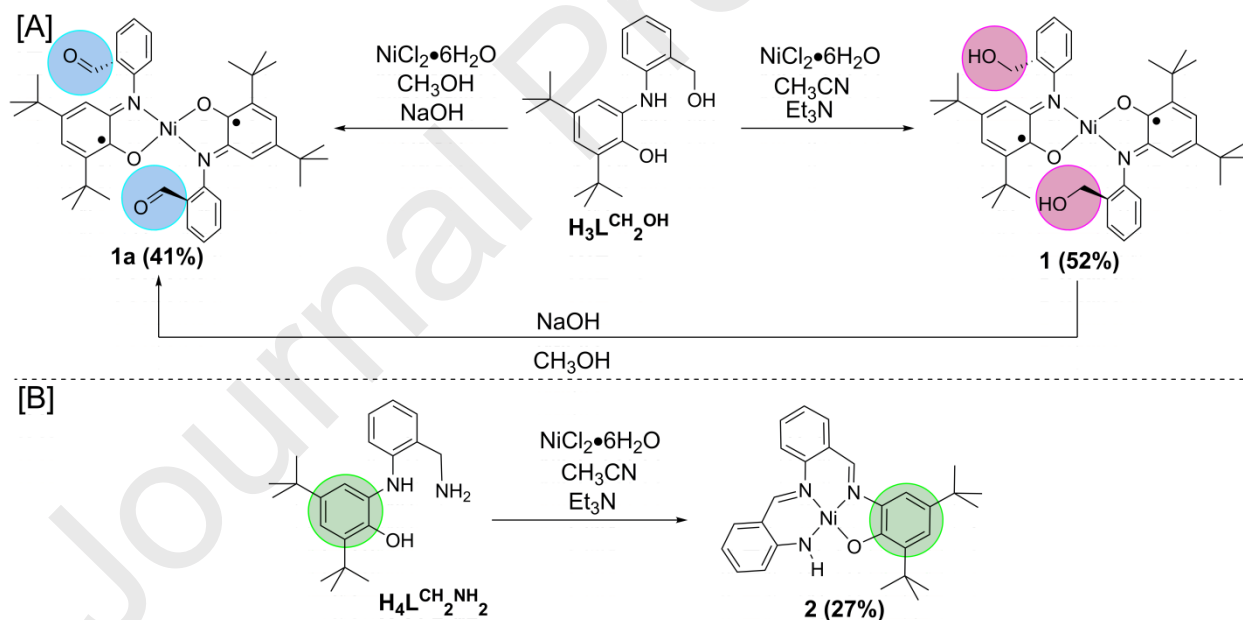
(4H, -CH₂), 6.17 (s, 1H, Ar-H), 6.23 (s, 1H, Ar-H), 6.91 (s, 2H, Ar-H), 7.26 (s, 2H, Ar-H), 7.35–7.51 (m, 4H, Ar-H), 7.60–7.62 (m, 2H, Ar-H) ppm. ¹³C NMR (CDCl₃, 100 MHz): δ 148.87, 146.34, 142.28, 135.42, 129.67, 129.18, 127.49, 125.64, 121.69, 121.55, 119.04, 114.20, 64.76, 35.02, 34.40, 31.64, 29.58 ppm. ESI-MS (CH₃CN) *m/z* for [C₄₂H₅₄N₂NiO₄]⁺: Calcd, 708.34; Found, 708.35. UV-Vis-NIR (CH₂Cl₂) λ_{max}, nm (ε, M⁻¹cm⁻¹): 890(35350), 590(2450), 470(3050).

Synthesis of [C₄₂H₅₀N₂NiO₄]; 1a; {[Ni^{II}(L^{CHO})₂]⁰}: To a stirred solution of ligand H₃L^{CH₂OH} (0.329 g, 1.0 mmol) and NiCl₂•6H₂O (0.120 g, 0.5 mmol) in methanol (5mL), was added a methanolic solution of NaOH (0.060 g in 20 mL methanol). Resulting solution was stirred for 1 h at room temperature (30 °C), caused a green precipitation. The precipitate was collected through filtration, washed with methanol. Recrystallization of this solid from dichloromethane:methanol (3:1) solvent mixture by slow solvent evaporation technique, provided the crystalline compound suitable for the single crystal X-ray diffraction analysis. Yield: 0.144 g, 0.20 mmol, 41%. FTIR (KBr pellet, cm⁻¹): 3075, 2955, 2900, 2866, 2751, 1691, 1592, 1571, 1534, 1522, 1473, 1450, 1437, 1361, 1323, 1286, 1257, 1228, 1199, 1174, 1155, 1106, 1095, 1025, 999, 919, 880, 873, 854, 837, 818, 672, 647, 636, 612, 590, 563, 543. ¹H NMR (CDCl₃, 399.85 MHz): δ 0.96 (s, 18H, *t*Bu), 1.06 (s, 18H, *t*Bu), 6.30 (d, 2H, *J* = 8.0 Hz, Ar-H), 6.92 (s, 2H, Ar-H), 7.57–7.64 (m, 6H, Ar-H), 8.08 (s, 2H, Ar-H), 10.75 (s, 1H, -CHO), 10.97 (s, 1H, -CHO) ppm. ¹³C NMR (CDCl₃, 100 MHz): δ 190.22, 189.63, 172.85, 172.63, 155.63, 155.29, 151.37, 151.25, 147.77, 141.16, 133.79, 133.46, 128.37, 127.13, 126.85, 112.74, 112.59, 34.95, 34.39, 30.41, 29.07 ppm. ESI-MS (CH₃CN) *m/z* for [C₄₂H₅₀N₂NiO₄]⁺: Calcd, 704.31; Found, 704.32. UV-Vis-NIR (CH₂Cl₂) λ_{max}, nm (ε, M⁻¹cm⁻¹): 900(42400), 590(2800), 388(7150).

Synthesis of [C₂₈H₃₁N₃NiO]; 2; {[Ni^{II}(HL3)]⁰}: Ligand H₄L^{CH₂NH₂} (0.326 g, 1.00 mmol) was treated with NiCl₂•6H₂O (0.239 g, 1 mmol) in acetonitrile (15 mL) in the presence of triethylamine (0.2 mL). The resulting reaction mixture was allowed to reflux for 3 h. After cooling to room temperature (30 °C), it was further stirred for 1.5 h. After that, the reaction mixture was filtered and washed with acetonitrile to get a red solid. Solid residue was recrystallized from dichloromethane:acetonitrile (3:1) solvent mixture. Yield: 0.065 g, 0.13 mmol, 27%. FTIR (KBr pellet, cm⁻¹): 3346, 3056, 2945, 2900, 2860, 1617, 1599, 1560, 1530, 1476,

1446, 1414, 1342, 1326, 1290, 1264, 1221, 1178, 1154, 1121, 850, 834, 746, 730, 677, 538, 457. ^1H NMR (CDCl_3 , 399.85 MHz): δ 1.35 (s, 9H, *t*Bu), 1.49 (s, 9H, *t*Bu), 5.97 (s, 1H, N-H), 6.51 (t, $J = 7.2$ Hz, 1H, Ar-H), 7.03 (d, $J = 8.4$ Hz, 1H, Ar-H), 7.15 (t, $J = 6.8$ Hz, 1H, Ar-H), 7.18 (s, 1H, Ar-H), 7.40 (t, $J = 7.6$ Hz, 2H, Ar-H), 7.46 (s, 1H, Ar-H), 7.55 (t, $J = 7.8$ Hz, 1H, Ar-H), 7.69 (d, $J = 8.0$ Hz, 1H, Ar-H), 7.82 (d, $J = 7.6$ Hz, 1H, Ar-H), 8.56 (s, 1H, $-\text{C}=\text{C}-\text{H}$), 8.73 (s, 1H, $-\text{C}=\text{C}-\text{H}$) ppm. ^{13}C NMR (CDCl_3 , 100 MHz): δ 163.08, 155.59, 152.73, 144.76, 143.68, 139.20, 138.38, 136.47, 133.33, 133.17, 132.62, 131.23, 124.79, 124.39, 124.31, 121.36, 120.23, 116.18, 114.60, 108.78, 35.14, 34.40, 31.89, 29.43 ppm. ESI-MS (CH_3CN) m/z for $[\text{C}_{28}\text{H}_{31}\text{N}_3\text{NiO} + \text{H}]^+$: Calcd, 484.19; Found, 484.20. UV-Vis-NIR (CH_2Cl_2) λ_{max} , nm (ϵ , $\text{M}^{-1}\text{cm}^{-1}$): 518(25100), 390(40200), 326(42050).

Results and Discussion



Scheme 2. Schematic representations for the syntheses of the complexes.

3,5-Di-*tert*-butylcatechol in a condensation reaction with an equimolar amount of 2-aminobenzonitrile or 2-aminobenzylalcohol in hexane, in the presence of triethylamine (Et_3N)

under air, provided ligand $\text{H}_2\text{L}^{\text{CN}}$ or $\text{H}_3\text{L}^{\text{CH}_2\text{OH}}$ in good yields.[25, 22] The reduction of $\text{H}_2\text{L}^{\text{CN}}$ using LiAlH_4 in dry THF under inert atmosphere yielded the expected ligand $\text{H}_4\text{L}^{\text{CH}_2\text{NH}_2}$. [23] In a 1.0:0.5 ratio reaction between ligand $\text{H}_3\text{L}^{\text{CH}_2\text{OH}}$ and $\text{NiCl}_2 \cdot 6\text{H}_2\text{O}$ in acetonitrile in the presence of Et_3N under air provided complex **1**. Upon changing the base to sodium hydroxide (NaOH), complex **1a** was formed under the same reaction condition in methanol (Scheme 2). In complex **1a**, the alcohol group was being oxidized to the aldehyde group. It is to note that complex **1a** can also be prepared starting from complex **1** by reacting with 3 equivalent amounts of NaOH in CH_3OH . Ligand $\text{H}_4\text{L}^{\text{CH}_2\text{NH}_2}$ upon reacting with an equivalent amount of $\text{NiCl}_2 \cdot 6\text{H}_2\text{O}$ in the presence of Et_3N under air provided complex **2** (Scheme 2). Noteworthy, the ligand backbone in complex **2** was completely different than the initially used $\text{H}_4\text{L}^{\text{CH}_2\text{NH}_2}$ ligand scaffold. The relocation in the position of 2,4-*di-tert*-butyl phenol unit from aniline N atom to benzyl amine N atom was warranted.

In the infrared (IR) spectrum of complex **1** a band at 3540 cm^{-1} was found, which implied the presence of free $-\text{OH}$ group in the complex. Interestingly, in complex **1a**, the band was absent and a new band at 1693 cm^{-1} was found due to the $\nu(\text{C}=\text{O})$ stretching of the $-\text{CHO}$ group. The IR spectrum of complex **2** exhibited a band at 3346 cm^{-1} due to asymmetric $\nu(\text{N}-\text{H})$ stretching. The asymmetric, symmetric, and bending overtone bands for $\nu(\text{C}-\text{H})$ stretches of *tert*-butyl groups were found at 2945 , 2860 , and 2900 cm^{-1} , while the corresponding bending vibrational band arose at 1476 cm^{-1} . Two bands appeared at 1617 , and 1599 cm^{-1} for two different $\nu(\text{C}=\text{N})$ stretching units. The phenolate $\nu(\text{C}-\text{O})$ band appeared at 1264 cm^{-1} .

The electrospray ionization (ESI) mass spectra of all the complexes were measured in the positive mode in CH_3CN solution. Complex **1** and complex **1a** showed a 100% molecular ion peak at $m/z = 708.35$, and 704.32 , respectively, corresponded to the $[\text{M}]^+$, while, complex **2** showed a 100% molecular ion peak at $m/z = 484.20$ that corresponded to $[\text{M} + \text{H}]^+$ (M stands for molecular mass). Isotope distribution pattern examination of the observed mass peaks revealed the composition as: $\text{C}_{42}\text{H}_{54}\text{NiN}_2\text{O}_4$ for complex **1**; $\text{C}_{42}\text{H}_{50}\text{NiN}_2\text{O}_4$ for complex **1a**; and $\text{C}_{28}\text{H}_{31}\text{N}_3\text{NiO}$ for complex **2** and supported the formation of the expected metal complexes.

Crystallographic Study

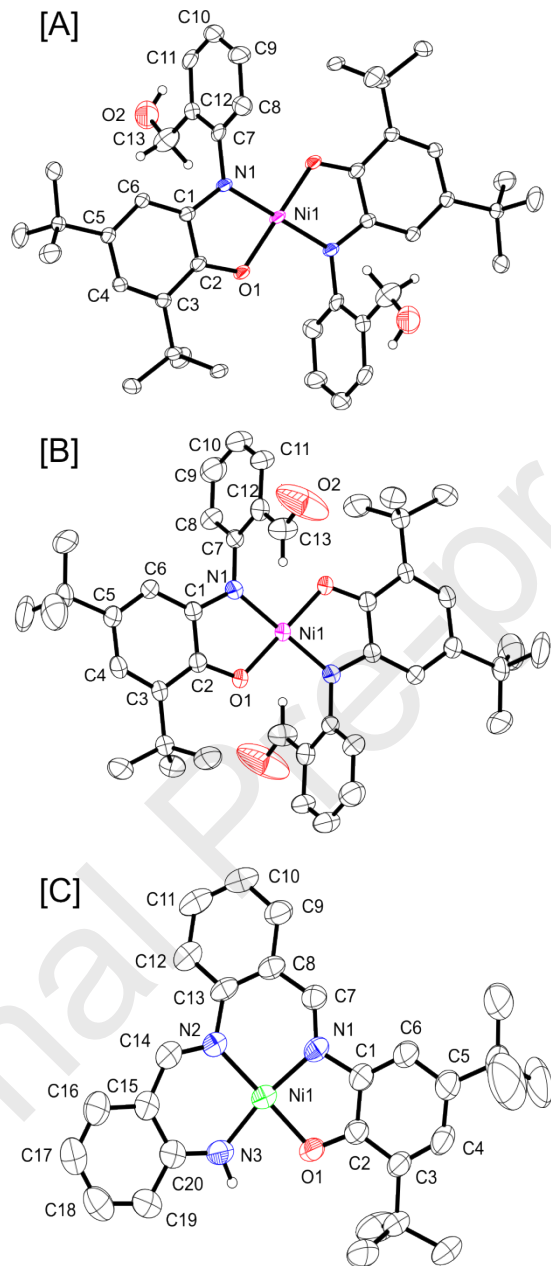


Figure 1. ORTEP diagrams for complexes **1** [A], **1a** [B], and **2** [C] were drawn at 40% thermal probability level. H atoms except attached with C13 (**1**, **1a**); O2 (**1**); and N3 (**2**) were omitted for clarity.

The molecular structures of all the complexes were investigated by X-ray single crystal diffraction measurements. Complex **1**, and complex **1a** crystallized in the triclinic space group $P\bar{1}$, while, complex **2** crystallized in the monoclinic space group $C2/c$. In complexes **1** and **2**, a

dianionic, fully reduced 2-amidophenolate [(AP)²⁻] form, the aromaticity of the C₆ ring prevails and C_{Ph}-N_{Ph}, and C_{Ph}-O_{Ph} exhibit single bond character (Chart 1). In case of one-electron oxidized iminosemiquinone {(ISQ^{•1-})} and two-electron oxidized iminobenzoquinone {(IBQ⁰)} forms, the aromaticity of the C₆ ring collapses and a quinoid-type distortion appears. Additionally, in the (IBQ⁰) form the C_{Ph}-N_{Ph}, and C_{Ph}-O_{Ph} are double bonds, while, the bonds are of intermediate between single and double bonds in (ISQ)¹⁻ form [Chart 1].

The C-C bond distances of the *tert*-butyl-containing phenyl rings were not within the range of 1.390 ± 0.001 Å as would be for a fully reduced 2-amidophenolate system. An alternating short-long-short bond distances {C3-C4 = 1.377(6) [**1**], 1.374(5) [**1a**] Å; C4-C5 = 1.433(6) [**1**], 1.431(6) [**1a**] Å; C5-C6 = 1.380(6) [**1**], 1.359(6) [**1a**] Å} followed by three long bonds (Table 2) were found. Such type of quinoid-type distortion indicated oxidation of the coordinated-ligands in the complexes. The C1-N1 and C2-O1 bond distances were 1.350(6) [**1**]; 1.347(5) [**1a**] Å and 1.316(6) [**1**]; 1.316(5) [**1a**] Å, respectively, and were in between their single bond and double bond characters. Thus, the coordinating ligands exist in their one-electron oxidized iminosemiquinone (ISQ^{•1-}) form. Hence, X-ray structural analysis concluded that both complex **1** and complex **1a** are Ni(II)-bis(iminosemiquinone) complexes.

In neutral complex **2**, the central Ni1 atom was four-coordinate with a slightly distorted square planar geometry ($\tau = 0.11$). [37, 38] The dihedral angle between N2-N1-N3 and N1-Ni1-O1 planes was 8.3° and indicated a small twist around the Ni atom in the molecule. An asymmetric environment around Ni1 atom was reflected by the Ni1-O1 = 1.858(2), Ni1-N1 = 1.867(3), Ni1-N2 = 1.876(3), and Ni1-N3 = 1.830(3) Å bond distances. The difference in the bond distances was due to the different nature (hybridization) of the coordinating atoms. The C-C bond distances of the *tert*-butyl groups-containing C₆ phenyl ring were almost all within 1.39 ± 0.02 Å range and were in accord with the phenyl C=C bond distances. [39-41] Furthermore, both C1-N1 = 1.417(5), O1-C2 = 1.321(4) Å bond distances implied their single bond character. These bond distances along with the double bond characterizing N1-C7 = 1.301(4) Å bond confirmed an iminophenolate form of the *tert*-butyl groups-containing phenyl ring where the PhO¹⁻ charge was located on the phenolate oxygen atom. The C-C bond distances in the C₆ ring comprised of C15-to-C20 atoms showed a substantial elongation in C15-C16 = 1.422(6), C20-C15 = 1.426(5), and C19-C20 = 1.424(6) Å bond distances compared to the C16-C17 =

1.357(6), C17–C18 = 1.398(6), C18–C19 = 1.365(6) Å and indicated a quinoid-type distortion in the C₆ ring. This distortion was due to the delocalization of amide negative charge over the iminosalicylidene moiety as evidenced by short N3–C20 = 1.327(5), and C14–C15 = 1.408(5) Å bond distances compared to their corresponding single bond characterizing values [42–44] followed by an elongated C14–N2 = 1.324(5) Å bond distance compared to its double bond characterizing value (1.28 Å).[45, 46] This type of alternative shortening and elongation is common in salen-type complexes where the ligand is found to be in its fully reduced form.[38–40] Hence, from the X-ray structural analysis it was clear that the neutral asymmetric complex **2** was Ni(II) salen-type with two imine N1 and N2 atoms, one amide N3 atom, and one phenolate O1 atom in its coordination environment.

Four-coordinate and square planar Ni(II)-bis(iminosemiquinone) complexes **1** and **1a** contained two radical-centered unpaired electrons. The electrons could render an $S = 1$ or $S = 0$ ground state owing ferromagnetic and antiferromagnetic coupling among them, respectively. In order to elucidate the electronic ground state of the complexes, ¹H-NMR measurements were performed (Figure S4–S5). NMR spectra as similar as that of ligand NMR spectra for both the complexes concluded diamagnetic nature with $S = 0$ electronic ground state. Thus, an antiferromagnetic coupling among the radical centers prevailed and the coupling was propagated *via* filled metal-centered t_{2g} orbitals.

Electrochemical Study

Cyclic voltammograms (CVs) for complexes **1**, **1a** and **2** were recorded in CH₂Cl₂, at a glassy carbon working electrode, and a Pt counter electrode under argon atmosphere. The CVs are depicted in Figure 2, Figure S16, Figure S17, Figure S18 and electron transfer potentials are presented in Table 2. Complex **1** showed one reversible two-electron oxidation, one reversible one-electron reduction and one irreversible reduction waves at -0.160, -0.965, and -1.640 V, respectively. Unlike complex **1**, complex **1a** exhibited two one-electron reversible oxidation waves at -0.133 V and 0.032 V, and one one-electron reversible reduction and one irreversible reduction processes at -0.936 V and -1.594 V, respectively. A possible structural change during one-electron oxidation, *i.e.*, the formation of a five-coordinate species by the coordination of an aldehyde unit in **1a**⁺, could be the reason for two one-electron processes. On increasing the scan rate from 50 mV/s to 500 mV/s, the peak separation between the two oxidation processes

diminished by 50 mV and supported the postulation. The CV of complex **2** represented irreversible electron transfer (oxidation) processes at 0.367 and 0.591 V. A quasi-reversible reduction occurred at -1.918 V. This could be the reduction of Ni(II) to Ni(I). [47]

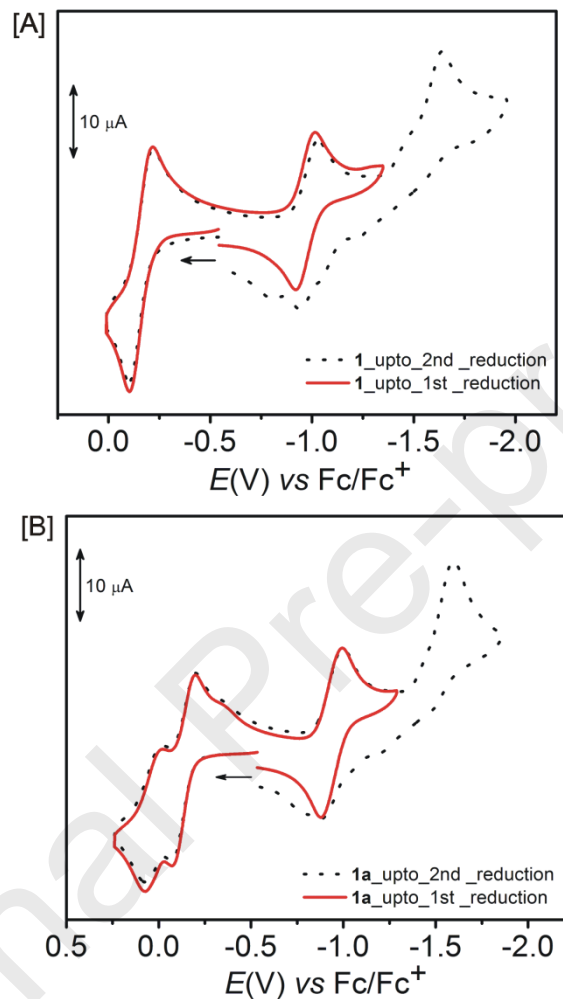


Figure 2. Cyclic voltammograms of complex **1** (A); and **1a** (B); measured at 100 mV/s.

Table 2. Voltammetric redox processes for complexes **1**, **1a**, and **2**.

Complex	E^0 , V			
	$E^{\text{red}2}$	$E_{1/2}^{\text{red}1}$	$E_{1/2}^{\text{ox}1}$	$E_{1/2}^{\text{ox}2}$
1	-1.640	-0.965	-0.160 ^a	
1a	-1.594	-0.936	-0.133	0.032
2		-1.918	0.367 ^b	0.591 ^b

a: 2e⁻ process; b: irreversible processes.

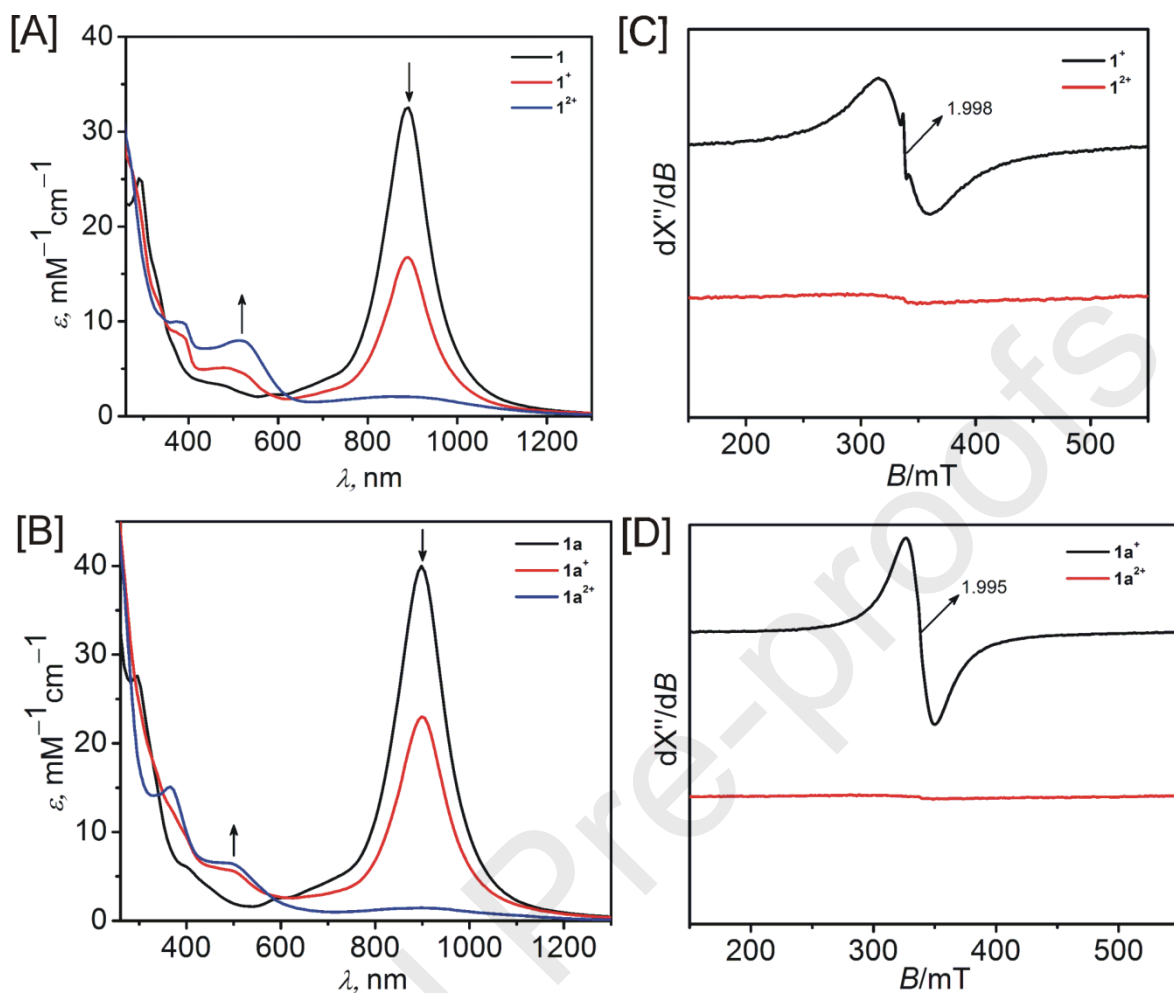


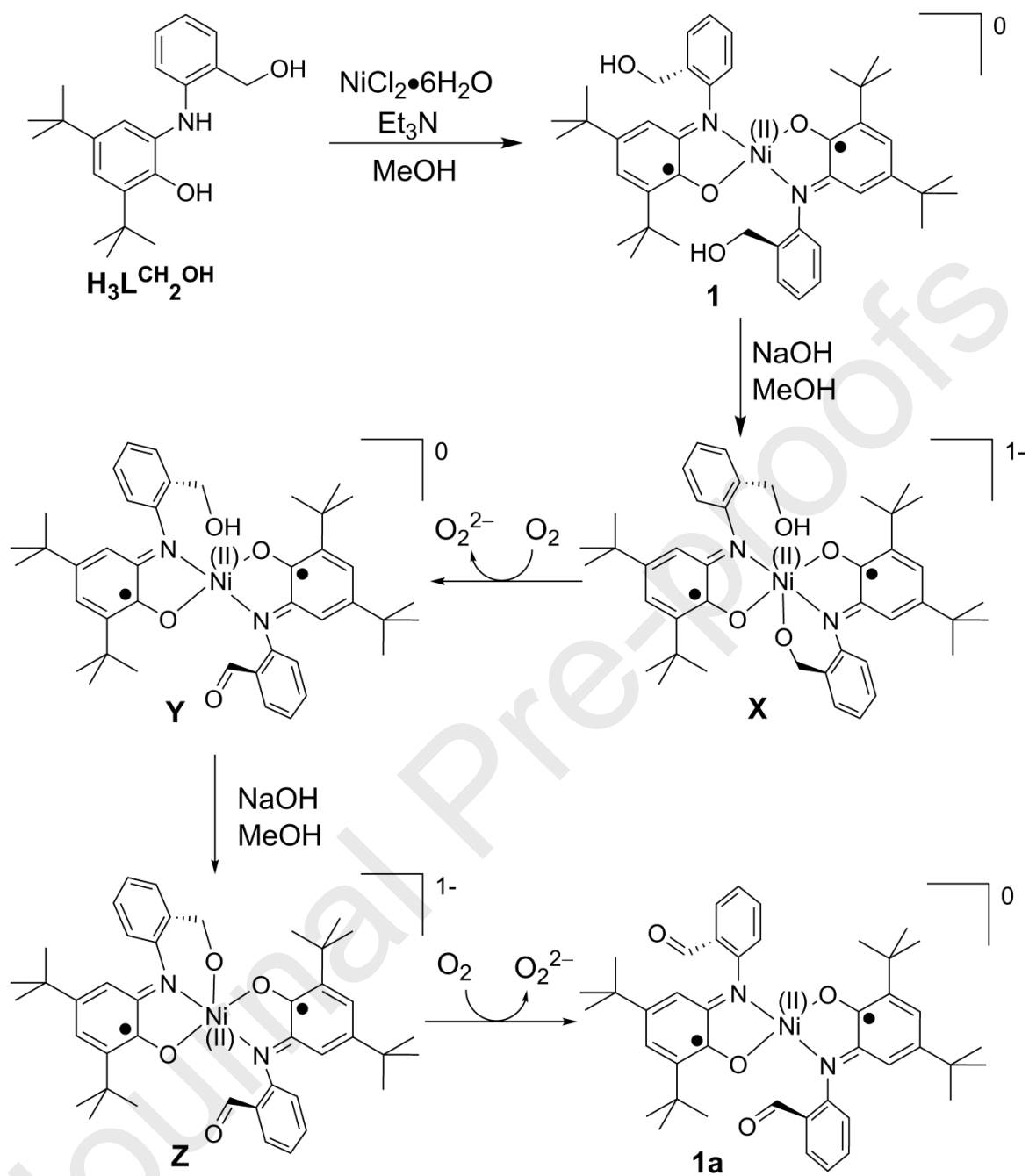
Figure 3. UV-Vis-NIR oxidation study of (A) **1**; (B) **1a** using acetylferrocenium hexafluorophosphate as the oxidant and ESR oxidation study of (C) **1** and (D) **1a** using acetylferrocenium hexafluorophosphate. X-band EPR spectra in CH_2Cl_2 solution. Conditions: temperature = 25 °C; microwave frequency = 9.446 GHz; modulation frequency = 100 kHz; modulation amplitude = 100.0 G; and microwave power = 0.995 mW.

Complex **1** and complex **1a** were oxidized chemically in CH_2Cl_2 using acetylferrocenium hexafluorophosphate as the oxidant. Upon addition of 1 equivalent amount of the oxidant the ligand-to-ligand charge transfer band [27, 48, 49] at 890 nm [**1**] and 900 nm [**1a**] diminished in intensity, while, a broad band, which could be assigned as ligand-based π - π^* charge transfer transitions of C=O and C=N units of an iminobenzoquinone moiety, [28] manifested at 516 nm [**1⁺**] and 506 nm [**1a⁺**]. Addition of another equivalent of the oxidant to the solutions, the ligand-to-ligand charge transfer band greatly reduced in intensity for complex **1⁺** and vanished for

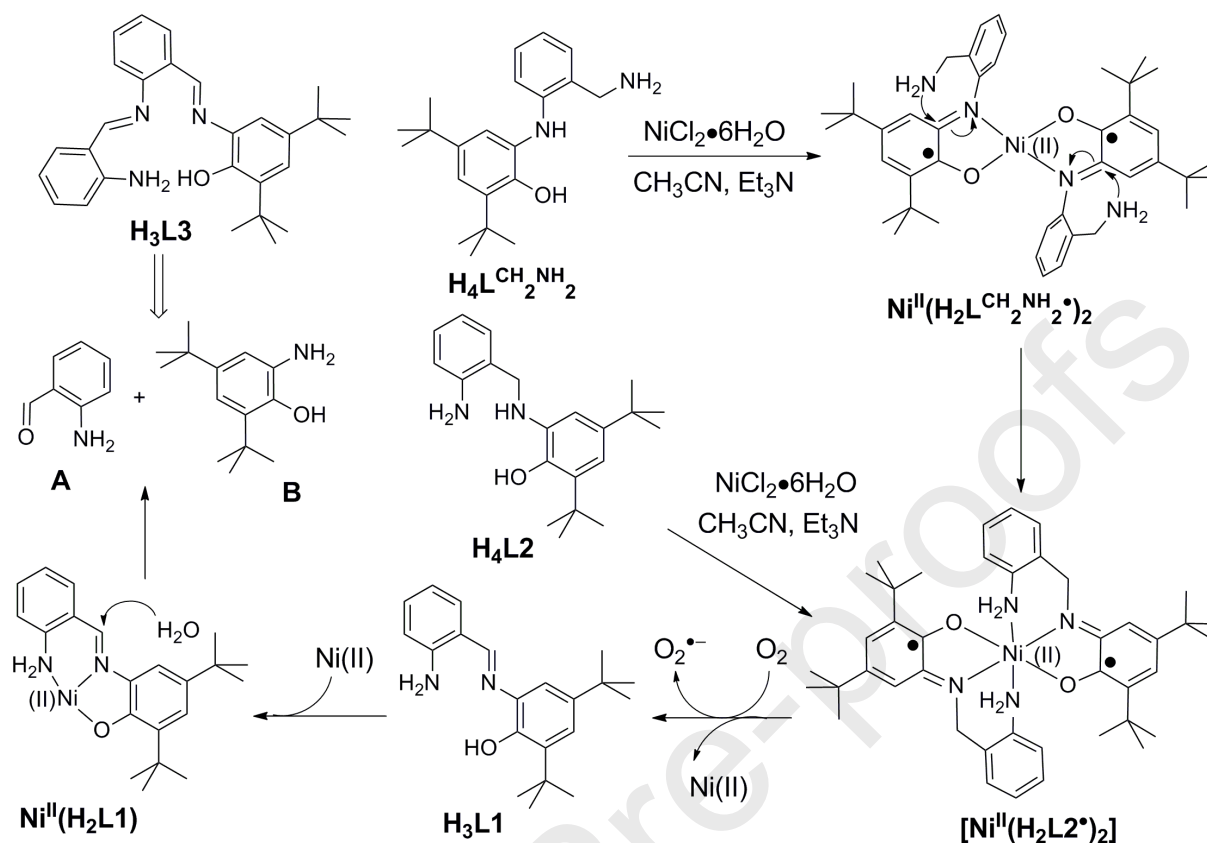
complex **1a**⁺. Further increase in the intensity of the broad band (506 nm) indicated the formation of iminobenzoquinone unit upon the oxidation. While, **1**²⁺ and **1a**²⁺ species were diamagnetic and did not show any X-band EPR spectrum, both **1**⁺ and **1a**⁺ rendered radical-based EPR signals { $g_{\text{iso}} = 1.998[\mathbf{1}^+]$, and $g_{\text{iso}} = 1.995[\mathbf{1a}^+]$ }. Thus, **1**⁺ and **1a**⁺ were Ni(II)-(iminosemiquinone)(iminobenzoquinone) species. In the case of complex **1**, which exhibited a two-electron oxidation process, assumed that in the presence of one equivalent amount of the oxidant 50% **1**²⁺ species was formed in the solution, initially. Thus formed species oxidized **1** by an electron and finally **1**⁺ existed in the solution, which provided the radical-based EPR signal.

Reactivity Study

Formation of two different complexes **1**, and **1a** from ligand $\text{H}_3\text{L}^{\text{CH}_2\text{OH}}$ depending on the employed base (Et_3N or NaOH) for the deprotonation of the ligands, implied that $\text{H}_3\text{L}^{\text{CH}_2\text{OH}}$ behaved as bidentate ligand in the presence of triethylamine, while, as a tridentate ligand in the presence of NaOH during the complexation process with $\text{NiCl}_2 \cdot 6\text{H}_2\text{O}$. Employment of a strong base like NaOH , ligand centered benzylic alcohol group ($-\text{CH}_2\text{OH}$) might be deprotonated to benzyloxy group ($-\text{CH}_2\text{O}^-$) and consequently, coordinated with the Ni(II) center. This caused lowering of the energy of benzylic C–H bonds enormously and easily oxidized to the aldehyde group by the coordinated–iminosemiquinone radical units as proposed for Cu–containing mononuclear metalloenzyme Galactose Oxidase. [50–52] Regeneration of Ni(II)–bis(iminosemiquinone) occurred by air. To find out the process of oxidative conversion of $-\text{CH}_2\text{OH}$ to $-\text{CHO}$ group, complex **1** was exposed to react with a methanolic solution of NaOH under air: eventually, complex **1a** was isolated. Therefore, by changing the basic strength, ligand flexibility (bidentate and tridentate nature of the ligand) can be altered, which controlled the different reactivity and thereafter, different product formation of $\text{H}_3\text{L}^{\text{CH}_2\text{OH}}$ ligand in the presence of $\text{NiCl}_2 \cdot 6\text{H}_2\text{O}$.



Scheme 3. Showing a mechanistic proposal for the conversion of **1a** from **1**.



Scheme 4. The mechanistic proposal for the formation of H_3L_3 from ligand $\text{H}_4\text{L}^{\text{CH}_2\text{NH}_2}$, and ligand H_4L_2 .

On the other hand, the formation of complex **2** from the initially used ligand $\text{H}_4\text{L}^{\text{CH}_2\text{NH}_2}$ via the *in situ* generation of ligand H_4L_2 and H_3L_1 and their corresponding Ni(II) complexes is presented in Scheme 4. Ligand $\text{H}_4\text{L}^{\text{CH}_2\text{NH}_2}$ initially reacted with $\text{NiCl}_2 \cdot 6\text{H}_2\text{O}$ in the presence of triethylamine and presumed to provide a diradical-coordinated square planar Ni(II) complex, $[\text{Ni}^{\text{II}}(\text{H}_2\text{L}^{\text{CH}_2\text{NH}_2\cdot})_2]$ (Scheme 4). Mass spectrometric analysis (Figure S11) of the reaction solution (CH_3CN), obtained after immediate mixing of the reactants $\text{H}_4\text{L}^{\text{CH}_2\text{NH}_2}$, $\text{NiCl}_2 \cdot 6\text{H}_2\text{O}$, and Et_3N under air, exhibited a mass peak at $m/z = 706.39$ that corresponded to $[\text{Ni}^{\text{II}}(\text{H}_2\text{L}^{\text{CH}_2\text{NH}_2\cdot})_2]$ species and supported its formation. The N atom from the free amine group of benzylamine then attacked at the imine carbon atom present in $[\text{Ni}^{\text{II}}(\text{H}_2\text{L}^{\text{CH}_2\text{NH}_2\cdot})_2]$ species. This resulted in the formation of an aryl migrated diradical-coordinated octahedral Ni(II) complex $[\text{Ni}^{\text{II}}(\text{H}_2\text{L}_2\cdot)_2]$ and complete modification of the initially used ligand backbone.

$[\text{Ni}^{\text{II}}(\text{H}_2\text{L}2^*)_2]$ underwent further two-electron aerial oxidation and provided two equivalents of organic ligand $\text{H}_3\text{L}1$, which upon coordination with $\text{Ni}(\text{II})$ ion provided $[\text{Ni}^{\text{II}}\text{H}_2\text{L}1]$ species (Scheme 4). The generated species then succumbed to ligand imine hydrolysis and provided 2-aminobenzaldehyde (**A**) and 4,6-di-*tert*-butyl-2-aminophenol (**B**). The coordination of imine N atom to Lewis acidic $\text{Ni}(\text{II})$ center activated the imine carbon atom by increasing its electrophilicity and hence, the hydrolysis occurred favorably. Thus *in situ* generated species **A**, and **B** upon condensation produced ligand $\text{H}_3\text{L}3$ and eventually, complex **2** was formed. The formation of complex **2** by using both $\text{H}_4\text{L}1$ [19] and $\text{H}_3\text{L}1$ [19] ligands supported the formation of the moieties as the intermediate metal-chelating units during the conversion of $\text{H}_4\text{L}^{\text{CH}_2\text{NH}_2}$ to $\text{H}_3\text{L}3$ under the reaction condition.

Conclusions

Ligand $\text{H}_3\text{L}^{\text{CH}_2\text{OH}}$ in the reaction with $\text{NiCl}_2 \cdot 6\text{H}_2\text{O}$ in the presence of triethylamine (Et_3N), as the base, under air, provided a regular four-coordinate $\text{Ni}(\text{II})$ -bis(iminosemiquinone) complex with a square planar geometry. In the complex, two $-\text{CH}_2\text{OH}$ units from two ligands remained far from the central $\text{Ni}(\text{II})$ ion and no $\text{Ni}-\text{O}(\text{alcohol})$ interaction was noticed. However, the deprotonation of the alcohol units by using stronger base NaOH , four-coordinate $\text{Ni}(\text{II})$ -bis(iminosemiquinone) complex was formed along with the oxidation of the alcohol units to aldehyde units. This implied a weak interaction between $\text{Ni}(\text{II})$ and $\text{O}(\text{alcoholate})$ atoms and thereafter, oxidation of benzyl alcoholate units took place with the participation of two metal-coordinated ligands-based radicals and air. Unlike ligand $\text{H}_3\text{L}^{\text{CH}_2\text{OH}}$, ligand $\text{H}_4\text{L}^{\text{CH}_2\text{NH}_2}$ provided a non-radical-containing four-coordinate salen-based $\text{Ni}(\text{II})$ complex. During the complex formation a complete relocation in the ligand backbone occurred where the 2,4-di-*tert*-butylphenol unit was migrated to the benzyl amine part from the aniline part. Hence, herein, instead of oxidation, a transimination took place.

Supplementary material: IR, NMR, Mass, CV and UV-vis/NIR, spectra of the complexes (**1**, **1a** and **2**); bond distances and bond angles tables for the complexes.

ACKNOWLEDGEMENT

This project is supported by SERB [EMR/2015/002491], Govt of India. GCP, MK and PS acknowledge Indian Institute of Technology Guwahati (IITG) for their doctoral fellowship. SG thanks CSIR–UGC for fellowship. FIST programme, DST, India, The Department of Chemistry, and CIF, IIT Guwahati are thankfully acknowledged for instrumental facility.

References

- [1] O. R. Luca, R. H. Crabtree, Redox-active ligands in catalysis, *Chem. Soc. Rev.*, 42(2013) 1440–1459.
- [2] J. I. van der Vlugt, Radical-Type Reactivity and Catalysis by Single-Electron Transfer to or from Redox-Active Ligands, *Chem. Eur. J.*, 25(2019) 2651–2662.
- [3] G. C. Paul, S. Ghorai, C. Mukherjee, Monoradical-containing four-coordinate Co(III) complexes: homolytic S–S and Se–Se bond cleavage and catalytic isocyanate to urea conversion under sunlight, *Chem. Commun.*, 53(2017) 8022–8025.
- [4] A. L. Smith, K. I. Hardcastle, J. D. Soper, Redox-Active Ligand-Mediated Oxidative Addition and Reductive Elimination at Square Planar Cobalt(III): Multielectron Reactions for Cross-Coupling, *J. Am. Chem. Soc.*, 132(2010) 14358–14360.
- [5] V. Lyaskovskyy, B. de Bruin, Redox Non-Innocent Ligands: Versatile New Tools to Control Catalytic Reactions, *ACS Catal.* 2(2012) 270–279.
- [6] S. K. Chatterjee, R. C. Maji, S. K. Barman, M. M. Olmstead, A. K. Patra, Hexacoordinate Nickel(II)/(III) Complexes that Mimic the Catalytic Cycle of Nickel Superoxide Dismutase, *Angew. Chem. Int. Ed.*, 53(2014) 10184–10189.
- [7] M. L. Kirka, D. A. Shultz, Transition metal complexes of donor–acceptor biradicals, *Coord. Chem. Rev.*, 257(2013) 218–233.
- [8] W. Kaim, B. Schwederski, Non-innocent ligands in bioinorganic chemistry—An overview, *Coord. Chem. Rev.*, 54(2010) 1580–1588.
- [9] P. J. Chirik, Preface: Forum on Redox-Active Ligands, *Inorg. Chem.*, 50(2011) 9737–9740.
- [10] A. I. Poddel'sky, V. K. Cherkasov, G. A. Abakumov, Transition metal complexes with bulky 4,6-di-*tert*-butyl-*N*-aryl(alkyl)-*o*-iminobenzoquinonato ligands: Structure, EPR and magnetism, *Coord. Chem. Rev.*, 253(2009) 291–324.

- [11] A. K. Dhara, K. Kumar, S. Kumari, U. P. Singh, K. Ghosh, Non-Innocent Property of Tridentate Ligand in Novel Cobalt Complex : Crystal Structure and Evidences for Cobalt(II) Phenoxy Radical Complex Formation, *ChemistrySelect*, 1(2016) 3933– 3937.
- [12] A. V. Piskunov, K. L. Pashanova, I. V. Ershova, A. S. Bogomyakov, A. G. Starikov, A. V. Cherkasov, Synthesis of four-, five-, and six-coordinate cobalt(III) bis-*o*-iminobenzosemiquinone complexes, *Russian Chemical Bulletin*, 68 (2019) 757–769.
- [13] A. V. Piskunov, I. N. Meshcheryakova, M. S. Piskunova, N. V. Somov, A. S. Bogomyakov, S. P. Kubrin, Diradical hexacoordinated tin(IV) bis-*o*-iminobenzosemiquinonates: synthesis, structure and magnetic properties, *Journal of Molecular structure*, 1195 (2019) 417–425.
- [14] E. Bill, E. Bothe, P. Chaudhuri, K. Chloplek, D. Herebian, S. Kokatam, K. Ray, T. Weyhermüller, F. Neese, K. Wieghardt, Molecular and Electronic Structure of Four- and Five-Coordinate Cobalt Complexes Containing Two *o*-Phenylenediamine- or Two *o*-Aminophenol-Type Ligands at Various Oxidation Levels: An Experimental, Density Functional, and Correlated *ab initio* Study, *Chem. Eur. J.*, 11 (2005) 204–224.
- [15] D. L. J. Broere, D. K. Modder, E. Blokker, M. A. Siegler, J. I. van der Vlugt, Metal-Metal Interactions in Heterobimetallic Complexes with Dinucleating Redox-Active Ligands, *Angew. Chem. Int. Ed.*, 55 (2016) 2406–2410.
- [16] C. Mukherjee, U. Pieper, E. Bothe, V. Bachler, E. Bill, T. Weyhermüller, P. Chaudhuri, Ligand-Derived Oxidase Activity. Catalytic Aerial Oxidation of Alcohols (Including Methanol) by Cu(II)-Diradical Complexes, *Inorg. Chem.*, 47(2008) 8943–8956.
- [17] Y. Ren, K. Cheaib, J. Jacquet, H. Vezin, L. Fensterbank, M. Orio, S. Blanchard, M. D. Murr, Copper-Catalyzed Aziridination with Redox-Active Ligands: Molecular Spin Catalysis, *Chem. Eur. J.*, 24(2018) 5086–5090.
- [18] D. L. J. Broere, B. de Bruin, J. N. H. Reek, M. Lutz, S. Dechert, J. I. van der Vlugt, Intramolecular Redox-Active Ligand-to-Substrate Single-Electron Transfer: Radical Reactivity with a Palladium(II) Complex, *J. Am. Chem. Soc.*, 136(2014) 11574–11577.
- [19] B. Bagh, D. L. J. Broere, V. Sinha, P. F. Kuijpers, N. P. van Leest, B. de Bruin, S. Demeshko, M. A. Siegler, J. I. van der Vlugt, Catalytic Synthesis of N-Heterocycles via Direct C(sp³)-H Amination Using an Air-Stable Iron(III) Species with a Redox-Active Ligand, *J. Am. Chem. Soc.*, 139(2017) 5117–5124.

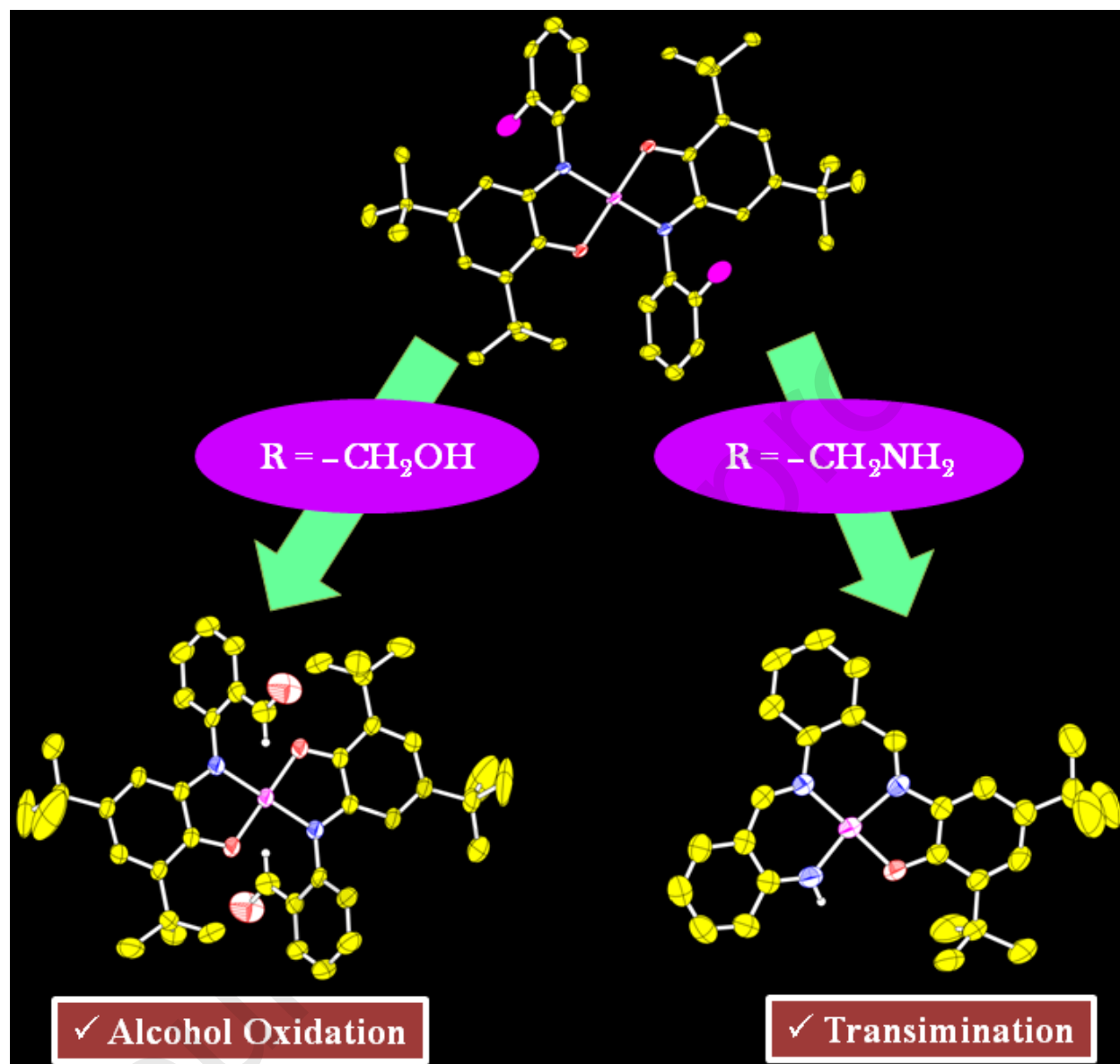
- [20] J. Jacquet, K. Cheaib, Y. Ren, H. Vezin, M. Orio, S. Blanchard, L. Fensterbank, M. D. Murr, Circumventing Intrinsic Metal Reactivity: Radical Generation with Redox-Active Ligands, *Chem. Eur. J.*, 23(2017) 15030–15034.
- [21] M. van der Meer, Y. Rechkemmer, I. Peremykin, S. Hohloch, J. van Slageren, B. Sarkar, (Electro)catalytic C–C bond formation reaction with a redox-active cobalt complex, *Chem. Commun.*, 50(2014) 11104–11106.
- [22] C. Mukherjee, T. Weyhermüller, E. Bothe, E. Rentschler, P. Chaudhuri, A Tetracopper(II)-Tetradentate Cuboidal Core and Its Reactivity as a Functional Model of Phenoxazinone Synthase, *Inorg. Chem.*, 46(2007) 9895–9905.
- [23] S. Ghorai, C. Mukherjee, Copper(II)-Mediated Transformation of a Tridentate Non-Innocent Ligand into a Tetradentate Salen-Type Innocent Ligand, *Chem. Asian J.*, 9(2014) 3518 – 3524.
- [24] G. M. Sheldrick, A short history of *SHELX*, *Acta Crystallogr.*, A64(2008) 112–122.
- [25] S. Ghorai, C. Mukherjee, Ortho-substituent induced triradical-containing tetranuclear oxovanadium(IV) cluster formation via ligand C–N bond breaking and C–O bond making, *Chem. Commun.*, 48(2012) 10180–10182.
- [26] A. Okuniewski, D. Rosiak, J. Chojnacki, B. Becker, Coordination polymers and molecular structures among complexes of mercury(II) halides with selected 1-benzoylthioureas, *Polyhedron*, 90(2015) 47–57.
- [27] P. Chaudhuri, C. N. Verani, E. Bill, E. Bothe, T. Weyhermüller, K. Wieghardt, Electronic Structure of Bis(*o*-iminobenzosemiquinonato)metal Complexes (Cu, Ni, Pd). The Art of Establishing Physical Oxidation States in Transition-Metal Complexes Containing Radical Ligands, *J. Am. Chem. Soc.*, 123(2001) 2213–2223.
- [28] A. Ali, D. Dhar, S. K. Barman, F. Lloret, R. Mukherjee, Nickel(II) complex of a hexadentate ligand with two *o*-iminosemiquinonato(1–) π -radical units and its monocation and dication, *Inorg. Chem.*, 55(2016) 5759–5771.
- [29] H. Chun, E. Bill, E. Bothe, T. Weyhermüller, K. Wieghardt, Octahedral (*cis*-Cyclam)iron(III) Complexes with *O,N*-Coordinated *o*-Iminosemiquinonate(1–) π Radicals and *o*-Imidophenolate(2–) Anions, *Inorg. Chem.*, 41(2002) 5091–5099.

- [30] H. Chun, P. Chaudhuri, T. Weyhermüller, K. Wieghardt, *o*-Iminobenzosemiquinonato Complexes of Mn(III) and Mn(IV). Synthesis and Characterization of $[\text{Mn}^{\text{III}}(\text{L}^{\text{ISQ}})_2(\text{L}^{\text{AP}})]$ ($S_{\text{t}} = 1$) and $[\text{Mn}^{\text{IV}}(\text{L}^{\text{ISQ}})_2(\text{L}^{\text{AP}}\text{-H})]$ ($S_{\text{t}} = 1/2$), *Inorg. Chem.*, 41(2002) 790–795.
- [31] R. Rakshit, S. Ghorai, S. Biswas, C. Mukherjee, Effect of Ligand Substituent Coordination on the Geometry and the Electronic Structure of Cu(II)-Diradical Complexes, *Inorg. Chem.*, 53(2014) 3333–3337.
- [32] P. Sarkar, M. K. Mondal, A. Sarmah, S. Maity, C. Mukherjee, An Iminosemiquinone-Coordinated Oxidovanadium(V) Complex: A Combined Experimental and Computational Study, *Inorg. Chem.*, 56(2017) 8068–8077.
- [33] A. I. Poddel'sky, V. K. Cherkasov, G. K. Fukin, M. P. Bubnov, L. G. Abakumova, G. A. Abakumov, New four- and five-coordinated complexes of cobalt with sterically hindered *o*-iminobenzoquinone ligands: synthesis and structure, *Inorg. Chim. Acta.*, 357(2004) 3632–3640.
- [34] S. N. Brown, Metrical Oxidation States of 2-Amidophenoxide and Catecholate Ligands: Structural Signatures of Metal–Ligand π Bonding in Potentially Noninnocent Ligands. *Inorg. Chem.*, 51(2012) 1251–1260.
- [35] M. Shit, S. Bera, S. Maity, T. Weyhermüller, P. Ghosh, Coordination of *o*-benzosemiquinonate, *o*-iminobenzosemiquinonate and aldimine anion radicals to oxidovanadium(IV), *New J. Chem.*, 41(2017) 4564–4572.
- [36] S. Mondal, S. Bera, S. Maity, P. Ghosh, Orthometalated *N*-(Benzophenoxazine)-*o*-aminophenol: Phenolatoversus Phenoxy States, *ACS Omega*, 3(2018) 13323–13334.
- [37] S. Blanchard, F. Neese, E. Bothe, E. Bill, T. Weyhermüller, K. Wieghardt, Square Planar vs Tetrahedral Coordination in Diamagnetic Complexes of Nickel(II) Containing Two Bidentate π -Radical Monoanions, *Inorg. Chem.*, 44(2005) 3636–3656.
- [38] H. Ohtsu, K. Tanaka, Equilibrium of Low- and High-Spin States of Ni(II) Complexes Controlled by the Donor Ability of the Bidentate Ligands, *Inorg. Chem.*, 43(2004) 3024–3030.
- [39] A. I. Poddel'sky, N. N. Vavilina, N. V. Somov, V. K. Cherkasov, G. A. Abakumov, Triethylantimony(V) complexes with bidentate *O,N*-, *O,O*- and tridentate *O,N,O'*-coordinating *o*-iminoquinonato/*o*-quinonato ligands: Synthesis, structure and some properties, *J. Organomet. Chem.*, 694 (2009) 3462–3469.

- [40] A. I. Poddel'sky, V. K. Cherkasov, G. A. Abakumov, Transition metal complexes with bulky 4,6-di-tert-butyl-N-aryl(alkyl)-*o* iminobenzoquinonatonoligands: Structure, EPR and magnetism, *Coord. Chem. Rev.*, 253 (2009) 291–324.
- [41] C. Mukherjee, T. Weyhermüller, K. Wieghardt, P. Chaudhuri, A trinuclear complex containing Mn^{II}Mn^{III}Mn^{IV}, radicals, quinine and chloride ligands potentially relevant to PS II, *Dalton Trans.*, (2006) 2169–2171.
- [42] C. Mukherjee, A. Stmmler, H. Bögge, T. Glaser, Do Trinuclear Triplesalen Complexes Exhibit Cooperative Effects? Synthesis, Characterization, and Enantioselective Catalytic Sulfoxidation by Chiral Trinuclear Fe^{III} Triplesalen Complexes, *Chem. Eur. J.*, 16 (2010) 10137–10149.
- [43] T. Glaser, M. Heidemeier, R. Föhlich, P. Hildebrandt, E. Bothe, E. Bill, Trinuclear nickel complexes with triplesalen ligands: simultaneous occurrence of mixed valence and valence tautomerism in the oxidized species, *Inorg. Chem.*, 44 (2005) 5467–5482.
- [44] O. Rotthaus, O. Jarjayes, F. Thomas, C. Philouze, C. P. D. Valle, E. S. Aman, J. L. Pierre, Fine Tuning of the Oxidation Locus, and Electron Transfer, in Nickel Complexes of Pro-Radical Ligands, *Chem.–Eur. J.*, 12 (2006) 2293–2302.
- [45] M. Asadi, K. A. Jamshid, A. H. Kyanfar, Synthesis, characterization and equilibrium study of the dinuclear adducts formation between nickel(II) Salen-type complexes with diorganotin(IV) dichlorides in chloroform, *Inorg. Chim. Acta.*, 360(2007), 1725–1730.
- [46] L. Benisvy, R. Kannappan, Y.-F. Song, S. Milikisyants, M. Huber, I. Mutikainen, U. Turpeinen, P. Gamez, L. Bernasconi, E. J. Baerends, F. Hartl, J. Reedijk, A square-planar nickel(II) monoradical complex with a bis(salicylidene)diamine ligand, *Eur. J. Inorg. Chem.*, 5(2007) 637–642.
- [47] Electro-oxidation and electro-reduction of some iron(II), cobalt(II) and nickel(II) polypyridyl complexes in acetonitrile, *J. Electroanal. Chem.*, 84(1977) 373–386.
- [48] K. Ray, T. Weyhermüller, F. Neese, K. Wieghardt, Electronic Structure of Square Planar Bis(benzene-1,2-dithiolato) metal Complexes [M(L)₂]^z (z = 2–, 1–, 0; M = Ni, Pd, Pt, Cu, Au): An Experimental, Density Functional, and Correlated ab Initio Study, *Inorg. Chem.*, 50(2005) 5345–5360.

- [49] A. Mukherjee, R. Mukherjee, Bidentate Coordination of a Potentially Tridentate Ligand. A Mononuclear Four-Coordinate Ni(II) Complex Supported by Two o-Iminobenzosemiquinonato Units, *Indian J. Chem.*, 504(2011) 484–490.
- [50] N. Ito, S. E. V. Phillips, C. Stevens, Z. B. Ogel, M. J. McPherson, J. N. Keen, K. D. S. Yadav, P. F. Knowless, Novel thioether bond revealed by a 1.7 Å crystal structure of galactose oxidase, *Nature*, 350(1991) 87–90.
- [51] J. W. Whittaker, Free Radical Catalysis by Galactose Oxidase, *Chem. Rev.*, 103(2003) 2347–2364.
- [52] Y. Wang, J. L. DuBois, B. Hedman, K. O. Hodgson, T. D. P. Stack, Catalytic Galactose Oxidase Models: Biomimetic Cu(II)-Phenoxy-Radical Reactivity, *Science*, 279(1998) 537–540.

Graphical Abstract



A Ni(II)-bis(iminosemiquinone) complex core exhibited GOase-like reactivity by oxidizing the ligand-based benzyl alcohol moiety to the corresponding aldehyde moiety in the presence of NaOH. However, a transimination was realized for ligand-based benzyl amine moiety.

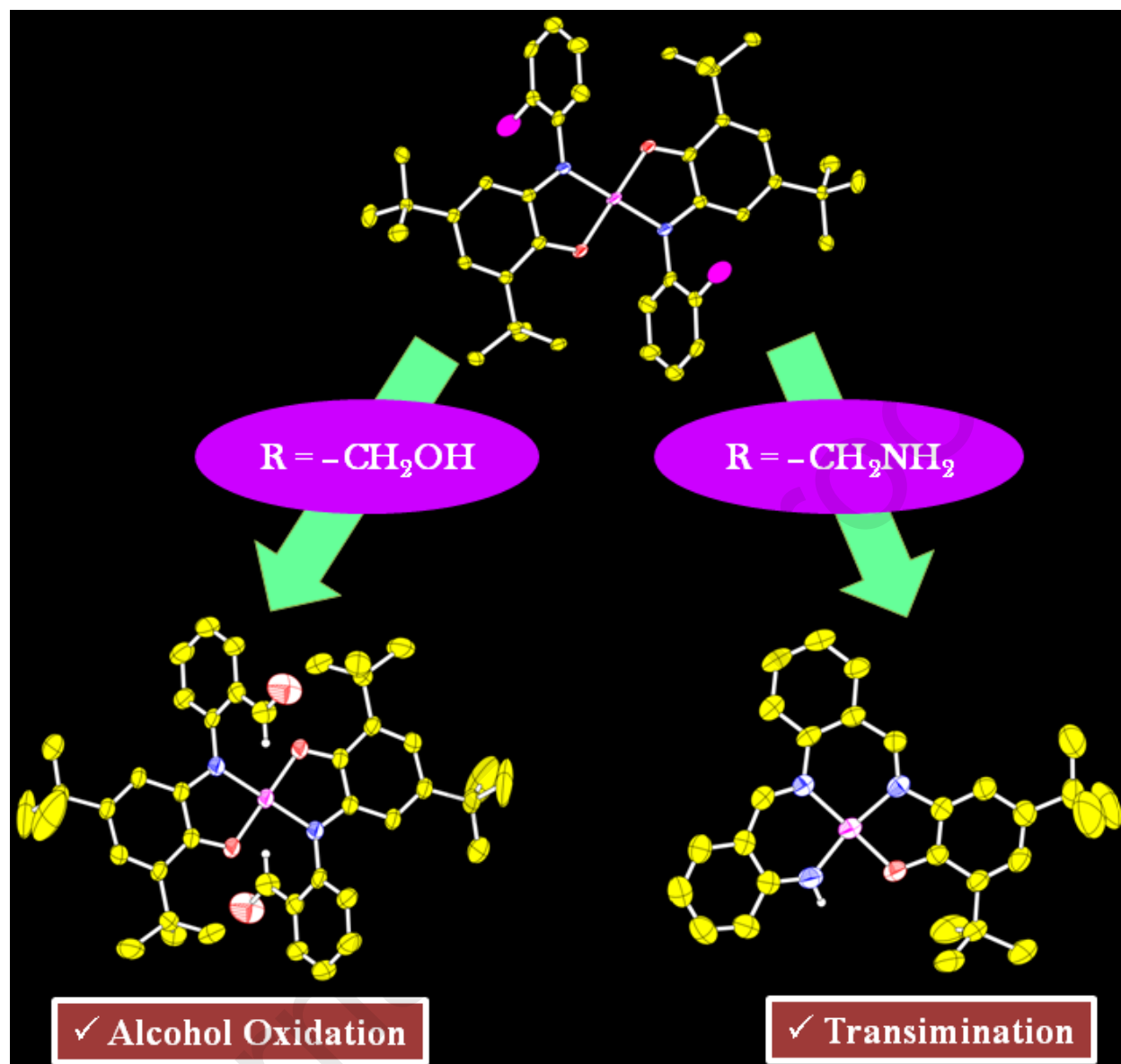
HIGHLIGHTS

- Oxidation of ligand-based benzyl alcohol units to benzaldehyde units by a Ni(II)-bis(iminosemiquinone) complex core.
- Transimination reaction in the presence of a ligand-based benzyl amine substituent in a Ni(II)-bis(iminosemiquinone) complex core.
- X-ray analyses of the complexes were done.
- Mechanistic investigation for the oxidation and the transimination were carried out.

Conflict of Interest

Authors have no Conflict of Interest.

Graphical Abstract



A Ni(II)-bis(iminosemiquinone) complex core exhibited GOase-like reactivity by oxidizing the ligand-based benzyl alcohol moiety to the corresponding aldehyde moiety in the presence of NaOH. However, a transamination was realized for ligand-based benzyl amine moiety.